Aberrant Functional Network Recruitment of Posterior Parietal Cortex in Turner Syndrome

Signe Bray,[1,2,3]* Fumiko Hoeft,[1,2] David S. Hong,[1,2] and Allan L. Reiss[1,2,4]

[1]*Center for Interdisciplinary Brain Science Research, Stanford University, Palo Alto, CA, USA*
[2]*Department of Psychiatry and Behavioral Sciences, Stanford University, Palo Alto, CA, USA*
[3]*Department of Psychiatry, Hotchkiss Brain Institute, University of Calgary, Calgary, AB, Canada*
[4]*Department of Radiology, Stanford University, Palo Alto, CA, USA*

Abstract: Turner syndrome is a genetic disorder caused by the complete or partial absence of an X chromosome in affected women. Individuals with TS show characteristic difficulties with executive functions, visual-spatial and mathematical cognition, with relatively intact verbal skills, and congruent abnormalities in structural development of the posterior parietal cortex (PPC). The functionally heterogeneous PPC has recently been investigated using connectivity-based clustering methods, which subdivide a given region into clusters of voxels showing similar structural or functional connectivity to other brain regions. In the present study, we extended this method to compare connectivity-based clustering between groups and investigate whether functional networks differentially recruit the PPC in TS. To this end, we parcellated the PPC into sub-regions based on temporal correlations with other regions of the brain. fMRI data were collected from 15 girls with TS and 14 typically developing (TD) girls, aged 7–14, while they performed a visual-spatial task. Temporal correlations between voxels in the PPC and a set of seed regions were calculated, and the PPC divided into clusters of voxels showing similar connectivity. It was found that in general the PPC parcellates similarly in TS and TD girls, but that regions in bilateral inferior parietal lobules, and posterior right superior parietal lobule, were reliably recruited by different networks in TS relative to TD participants. These regions showed weaker correlation in TS with a set of regions involved in visual processing. These results suggest that abnormal development of visuospatial functional networks in TS may relate to the well documented cognitive difficulties in this disorder. Hum Brain Mapp 00:000–000, 2012.

Key words: Turner syndrome; posterior parietal; functional connectivity

INTRODUCTION

Turner syndrome (TS) is a relatively common genetic disorder (~ 1 in 2000 live female births [Stochholm et al., 2006]) caused by the complete or partial absence of an X-chromosome in affected females. Individuals with TS typically present with short stature [Lippe, 1991], gonadal dysgenesis, estrogen insufficiency, and are at risk for cardiac malformations [Mazzanti and Cacciari, 1998]. The most common karyotype in individuals with TS is X monosomy (45, X), however, other karyotypes also occur in persons receiving this diagnosis, though they are associated with more variability in phenotypic features.

In terms of cognitive function, individuals with TS are typically in the normal range for full-scale IQ, but show relative weaknesses in mathematical, visuospatial, and executive functions, including working memory tasks, with relatively intact scores on measures of verbal function [Hong et al., 2009]. Several studies have also documented

*Correspondence to: Signe Bray, Department of Psychiatry and Hotchkiss Brain Institute, University of Calgary, Foothill Medical Center TRW 4D57. E-mail: slbray@ucalgary.ca

Received for publication 4 January 2012; Revised 28 March 2012; Accepted 24 April 2012

DOI: 10.1002/hbm.22131

Published online in Wiley Online Library (wileyonlinelibrary.com).

difficulties in social functioning in TS [Lawrence et al., 2003]. As a relatively common neurogenetic disorder, TS offers a unique opportunity to study the influence of X-chromosome genes and associated hormonal deficiency on brain and cognitive development.

In vivo magnetic resonance imaging (MRI) studies have identified several brain regions which appear to develop abnormally in TS (reviewed in [Raznahan et al., 2010]). The orbitofrontal cortex, insula [Marzelli et al., 2011], amygdala [Good et al., 2003], and superior temporal lobes [Marzelli et al., 2011] have all been found to show anatomical differences between TS and typically developing (TD) controls. These findings are interesting in light of the observed difficulties in the social domain in TS [Lawrence et al., 2003]. One of the most consistently observed differences has been abnormal morphology of the parietal lobes, including reductions in gray [Brown et al., 2002; Cutter et al., 2006; Molko et al., 2003, 2004] and white matter [Cutter et al., 2006; Holzapfel et al., 2006; Molko et al., 2004] volumes along the intraparietal sulcus, in both superior and inferior parietal cortex. Cortical regions along the intraparietal sulcus have been implicated in visuospatial [Silver and Kastner, 2009], auditory [Lewis et al., 2000] and tactile attention [Swisher et al., 2007], numerical cognition [Knops et al., 2009], visual short-term memory capacity [Todd and Marois, 2004], and memory retrieval processes [Nelson et al., 2010]. Abnormal parietal cortex morphology in TS has been presumed to relate to the cognitive difficulties in these domains.

Posterior parietal cortex (PPC) includes several anatomically defined regions including the superior and inferior parietal lobules (SPL and IPL); IPL can be further partitioned into angular and supramarginal gyri. However, given the involvement of this region in a wide array of functions, there has been recent interest in subdividing the parietal cortex into functional sub-units. It is logical that the functionality of a given brain region should relate to the connections it makes with other regions, and based on this principle several recent studies have used anatomical or functional connectivity to parcellate the PPC into distinct sub-regions [Anderson et al., 2010; Mars et al., 2011; Nelson et al., 2010], or explore the connectivity of anatomically defined sub-regions [Uddin et al., 2010]. Anderson et al. [2010] used connectivity measures derived from resting-state functional magnetic resonance imaging (fMRI) to divide the PPC into clusters of voxels showing similar connectivity to a set of pre-defined brain regions in the task-positive or attention network [Fox et al., 2005]. They identified IPS sub-regions that showed distinct connectivity with visual, auditory, somatosensory, and default-mode network regions, indicating functional specialization. Mars et al. [2011] used diffusion tractography to define clusters of parietal voxels with similar structural connectivity to the rest of the brain. To interrogate the function of these clusters, they defined a set of target regions, and calculated the correlation between time-series from these targets and the parietal clusters, during resting scans. These correlation-based maps were then compared against the diffusion-based parcellation, to gain insight into functional specialization of identified sub-regions. Nelson et al. [Nelson et al., 2010] used resting state connectivity to parcellate lateral parietal cortex into sub-regions, which were then compared in terms of involvement in memory retrieval processes, and whole-brain network membership.

Given that the PPC seems to develop abnormally in TS, and differences have also been observed in white matter volume and integrity in this region [Holzapfel et al., 2006; Yamagata et al., 2011], functional networks recruiting the PPC may also be affected in this condition [Honey et al., 2007]. A recent study from our group found that fronto-parietal functional connectivity is reduced in TS during working memory tasks [Bray et al., 2011]. However, it remains unknown how the multiple functional networks recruiting the PPC may be affected in TS. A detailed investigation of PPC functional networks in TS may provide additional insight into the consequences of abnormal development of the PPC, and could serve to bridge our understanding of the relationship between the observed differences in parietal morphology to the observed cognitive difficulties in TS.

In the present study, a connectivity-based parcellation of the PPC was performed in a group of pre-adolescent girls with TS, and a group of age-matched TD controls. Participants were scanned with fMRI while they performed a visual-spatial task in a blocked design. Bilateral PPC was divided into clusters of voxels showing similar connectivity profiles to a network of regions recruited by this task. Voxel-wise comparisons were then used to identify regions that consistently belonged to different clusters in TS relative to TD group. Given the cognitive profile in TS, we hypothesized that networks involved in visuospatial processing, and executive function, may show differences in TS.

METHODS

Participants and Recruitment

Participants in this study ranged from 7 to 14 years of age and were recruited as part of a study on brain and cognitive development in Turner syndrome. All TS participants included in this analysis were monosomic (45, X), and demonstrated 20–30 cells with X monosomy on standard karyotype assessment to confirm the diagnosis. TS girls were recruited from chapters of the Turner Syndrome Society of America and the Turner Syndrome Society of Canada, and from university and community based pediatric endocrinologists. TD participants were recruited as siblings of TS participants, and locally through parent organizations and advertisements in Palo Alto, CA. Study participation required 2 days of interviews and MRI scans at Stanford University.

AQ1

Experimental Protocol

Before MRI scanning, participants underwent a "mock scan session" in an MRI simulator, to familiarize themselves with the scanner environment, and to rehearse staying still during scanning. Study participants underwent two scan sessions, each up to 1.5 h, on consecutive days. On the first day, structural MRI and DTI scans were collected, as well as three fMRI task scans, presented in pseudo-random order. On the second day, participants performed three additional fMRI task scans, and repeated any scans that were inadequately collected on the first day. Among the functional tasks was the judgment of line orientation task described here, in addition to other tasks reported elsewhere. In addition to functional and structural MRI scans, participants underwent a battery of cognitive and neuropsychological tests. Informed consent was obtained from a family member, and informed assent was obtained from all participants. The human subjects committee at Stanford University School of Medicine approved the protocols used in this study.

Cognitive and Neuropsychological Assessments

To compare our participant groups on standardized measures of working memory, visuospatial, and verbal processing, we administered the Wechsler Intelligence Scale for Children, Fourth Edition (WISC-IV) [Wechsler, 2003] to all study participants. In addition to full-scale IQ [Wechsler, 2003], we report index scores from the WISC-IV for the verbal comprehension, perceptual reasoning, working memory, and processing speed indexes. Scores were compared between groups using univariate general linear models, including diagnosis as a factor and age as a centered covariate.

Participant Characteristics

35 TS (45, X) and 23 TD participants (all female) performed the judgment of line orientation (JLO) task reported here. Participants who performed below 85% accuracy on the easy experimental condition (see below for details), or whose scans were contaminated with excessive motion or scanner artifact, were excluded from our analysis. 18 TS and 2 TD participants were excluded for failing to meet the behavioral performance threshold, 5 TD and 2 TS participants were excluded due to image artifacts, and two additional TD participants were excluded due to excessive motion. A final group of 15 TS and 14 TD participants were included in the analyses reported here. Mean age (SD) for TS participants was 10.67 (2.0) and for TD participants 10.17 (2.1). TS participants had significantly lower full-scale IQ [TS mean: 94 (15); TD mean: 117 (12.5); F (1, 24) = 16.5, $P < 0.001$], as well as significantly lower scores on the working memory [TS mean: 85.1 (12); TD mean: 104.8 (12.2); F (1, 24) = 15.4, $P < 0.001$], processing speed [TS mean: 94 (12); TD mean: 113 (12.5); F (1, 24) = 14, $P < 0.001$], and perceptual reasoning [TS mean: 95 (14); TD mean: 117 (10.7); F (1, 24) = 18, $P < 0.001$] indices from the WISC-IV. Although significant differences were also observed on the verbal comprehension score, consistent with previous studies in TS, the mean difference in scores was narrower for this index [TS mean: 102 (18); TD mean: 115.8 (16); F (1, 24) = 4.6, $P = 0.04$].

MRI Data Acquisition

Magnetic resonance imaging was performed on a 3.0 T GE whole-body scanner (GE Healthcare Systems, Milwaukee, WI). High resolution structural scans were acquired using a spoiled GRASS sequence (124 slices, 0.86-mm^2 in-plane and 1.5-mm through-plane resolution, flip angle = 15°, FOV = 22 cm), facilitating subsequent localization and coregistration of functional data. A T2*-sensitive gradient echo spiral-in/out pulse sequence [Glover and Law, 2001] was used for functional imaging (TR = 2000 ms, TE = 30 ms, flip angle = 80°, matrix 64 × 64, FOV = 22 cm). Thirty oblique axial slices were obtained parallel to the AC-PC with 4-mm slice thickness, 1-mm skip. A high-order shimming procedure was used to reduce B0 heterogeneity before the functional scans [Kim et al., 2002].

Judgment of Line Orientation Task

Visual stimuli were controlled using ePrime software on a PC, and presented to participants in the scanner using a projector positioned at the front of the room; the image reflected off a mirror attached to the fMRI headcoil.

The task was a variation of Benton's judgment of line orientation (JLO) task [Benton et al., 1978], a test of visuospatial perceptual skills. The implementation of the task used in this study consisted of rest (R), experimental easy (EE), control easy (CE), experimental difficult (ED), and control difficult (CD) blocks presented in the following order: R-EE-CE-EE-CE-EE-CE-R-ED-CD-ED-CD-ED-CD-R. During the experimental tasks, participants were shown a protractor with 5 (easy) or 11 (difficult) lines arranged in the shape of a protractor (Fig. 1a,b). Two of the lines were highlighted in yellow, whereas the others were colored magenta. Two angled lines were presented at the bottom of the screen, and participants were asked to compare these lines with the lines highlighted above, and press a button if the two sets of lines matched. During the "difficult" task blocks, shortened line segments were shown (Fig. 1b). During the control task, three (easy) or five (difficult) parallel lines were shown at the bottom of the screen, in either yellow or magenta, and participants were asked to press a button if the color of the lines at the bottom of the screen matched the color of the lines in the protractor at the top of the screen (Fig. 1c).

Each rest epoch lasted 30 s, during which participants passively viewed a blank screen. Control (or "baseline") blocks began with a 4 s display of the instructions "judge

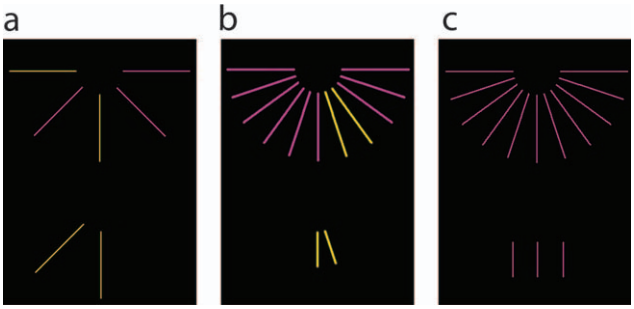

Figure 1.

Judgment of line orientation task. (**a**) Easy version of the task (low cognitive load). Participants press a button if the yellow lines at the bottom of the screen are in the same positions as the lines highlighted in yellow in the protractor at the top of the screen. (**b**) Difficult version of the task (high cognitive load). The task here is the same as the easy version, but there are 11 lines in the protractor and line segments on the bottom are shortened. (**c**) Control task in which participants are asked to press the button if the colors of the lines on the bottom match the lines on top. [Color figure can be viewed in the online issue, which is available at wileyonlinelibrary.com.]

if colors match." Experimental blocks began with a 4 s display of the instructions "judge if line orientations equal." Each baseline and experimental block consisted of 10 trials presented for 2500 ms each, with a 500 ms interstimulus interval.

Behavioral Data Analysis

Accuracy measures from the JLO task were entered into a repeated measures ANOVA, with level of difficulty (control/easy/difficult) as within subject factors, diagnosis as a between subjects factor, and age as a centered covariate.

fMRI Preprocessing

Functional images were pre-processed using SPM8 software (http://www.fil.ion.ucl.ac.uk/spm/software/spm8/) in MATLAB (Mathworks, Natick, MA). Images were corrected for slice-timing, realigned to the third scan in each functional series, and coregistered to the corresponding structural scan. We used ArtRepair software (http://cibsr.stanford.edu/tools/ArtRepair/ArtRepair.htm) to improve signal quality losses due to participant motion and data artifacts [Mazaika et al., 2009]. Artifacts indicated by rapid scan-to-scan motion greater than 0.5 mm/TR or global signal intensity fluctuations greater than 1.5% were repaired using interpolation between the nearest unrepaired scans. Participants were removed from further analysis if more than 25% of scans required repairs. Among participants included in the analyses reported here, the average number of scans repaired was 17 in the TD group and 16 in the TS group, with no significant difference between groups ($P = 0.87$). Images were normalized to the EPI template included in SPM, and smoothed with an 8 mm FWHM Gaussian kernel. For connectivity clustering analyses, residuals were obtained by regressing out the motion parameter estimates, as well as the average white matter and CSF time courses, and a linear trend to model signal drift over time. To obtain representative time courses from white matter and CSF, T1 images for each participant were registered to the functional images and segmented using automated procedures implemented in SPM8; time-courses were then extracted by averaging over voxels classified as belonging 100% to each tissue class (to exclude voxels near the gray/white matter interface).

SPM Analysis and ROI Generation

For each participant, we constructed a general linear model with regressors for the easy and difficult JLO task blocks, as well as for the control blocks, and a constant term. The task regressors were modeled as 30 s boxcar functions convolved with the hemodynamic response function, and a 128 s high-pass filter was applied. Task versus control contrasts for easy, difficult, and easy+difficult conditions were calculated and entered into group level two-sample *t*-tests to compare TD and TS groups.

To generate a set of regions with which parietal cortex connectivity could be tested, regions that were modulated by any of the task conditions across the entire group (TD+TS) were calculated. Specifically, for each participant, contrasts for each task regressor were calculated against an implicit baseline. These contrast images were then entered into a factorial model at the group level, with participants from both diagnostic groups pooled together. From this model an effect of interest F-contrast was calculated across the entire sample, intended to identify regions that were positively or negatively modulated by any of the task conditions. Target regions of interest (ROI) for the subsequent clustering analysis were chosen by thresholding the F-contrast map at a level of $P < 0.0001$ uncorrected with a minimum cluster size of 25 voxels. This yielded 19 peaks in gray matter bilaterally across the cortex, excluding peaks in white matter, cerebellum (as coverage of this region was uneven across participants) and the parietal lobes (listed in Table I); effectively this yielded a set of regions typically associated with attentional processing (SMA, bilateral FEF, bilateral insula, dorsal PFC, etc.). Cubic ROIs were generated as 10 mm^3 around these peaks; this set of ROIs will henceforth be referred to as the "target ROI mask."

Connectivity-Clustering Analysis

First, an ROI consisting of bilateral superior and inferior parietal cortex (bilateral PPC ROI), as defined in the AAL atlas [Tzourio-Mazoyer et al., 2002], was chosen as the volume to be sub-divided into clusters. Second, a target ROI

TABLE I. Peak locations included in seed ROI mask

Description	MNI coordinates		
	x	*y*	*z*
Right Inferior Temporal Gyrus/Lateral Occipital	48	−68	−6
Right cuneus	4	−80	30
Right Superior Frontal Gyrus	26	−6	58
Left Superior Frontal Gyrus	−24	−6	58
Right Precentral Gyrus	48	2	28
Right Middle Temporal Gyrus	68	−46	8
Right Middle Temporal Gyrus	60	−18	−10
Right Superior Temporal Gyrus	54	−8	−14
Left Precentral Gyrus	−52	2	30
Left Superior Frontal Gyrus	−18	58	4
Left Middle Temporal Gyrus	−54	−46	0
Right SMA	8	22	48
Left SMA	−8	16	48
Left Insula	−34	18	6
Left Fusiform Gyrus	−36	−48	−20
Right Middle Frontal Gyrus	42	34	36
Right Middle Frontal Gyrus	48	42	20
Right Operculum	54	−8	14
Right Superior Medial Gyrus	10	58	2

mask was chosen, as described earlier. The bilateral PPC ROI was then divided into clusters of voxels showing similar connectivity with the voxels in the target ROI mask. To do this, for each participant the temporal correlation between each parietal ROI voxel and each voxel in the target ROI mask, across the entire experimental time course, was calculated. This yielded an $n \times p$ matrix, where n is the number of voxels in the bilateral PPC ROI (1214), and p is the number of voxels in the target ROI mask (484). This matrix was then entered into k-means clustering, as implemented in MATLAB, and divided into clusters using a random starting point. With k-means clustering, the number of clusters is specified by the user, and in this study we tested cluster numbers from 3 to 10, based on the previous literature [Anderson et al., 2010; Mars et al., 2011]. To encourage consistency across the group, a two-pass procedure was implemented, in which the results from the first-pass of clustering were compared at the group level, to determine the cluster centers which best represented the group. Specifically, cluster centers from all individuals were binned together, such that the total distance to center at the group level was minimized. A set of cluster centers was calculated from the group mean, and then used to seed a second pass of the clustering algorithm.

Maps of parietal cortex were created in which each voxel reflected the proportion of participants from each group for whom that voxel belonged to a particular cluster. This enabled comparisons between diagnostic groups, using fisher's exact test for binomial distributions. Inferences were drawn at a significance level of $P < 0.05$. We additionally imposed a cluster-size threshold using a permutation analysis in which we randomly permuted participant labels 1000 times, and compared cluster sizes from the true labeling against the resulting distribution.

Cluster numbers from 3 to 10 were tested here; as the number of clusters increased, the spatial consistency across participants decreased. We were primarily interested in comparing cluster extent between groups, and therefore we report only clusterings that were consistent across the group. We report results from 3 to 6 clusters; 6 was the largest number of clusters for which all clusters had voxels engaged by the majority of participants, operationalized here as 60% of participants.

To ascertain that the functional connectivity of identified clusters was indeed distinct, representative time-courses from each cluster were extracted and entered into a whole-brain regression analysis. Time courses were obtained by averaging over voxels included in the cluster, after regressing out task-effects; whole brain regression models included task as well as motion regressors. This analysis identified which regions of the brain significantly correlated with each cluster. These analyses were performed across the entire group (TD + TS), and thresholded at $P < 0.05$ FWE whole-brain corrected.

Several regions showed group differences in cluster membership for 3, 4, 5, and 6 cluster divisions. To probe the source of these differences, whole-brain connectivity for these regions was compared, by entering voxel time courses into a whole-brain regression and comparing groups using two-sample *t*-tests. These regions were expected to show some group differences in regional correlations, but as this analysis was exploratory, a threshold of $P < 0.001$ uncorrected was employed.

RESULTS

JLO Performance

In the TD group, the average accuracy was 99%, 95%, and 55%, for the control, easy, and hard tasks, respectively. In the TS group the average accuracy was 93%, 92%, and 47%. A repeated measures ANOVA with difficulty as a within-subjects factor, diagnosis as a between-subjects factor, and age as a centered covariate showed that performance decreased with increasing difficulty [$F(2, 52) = 122$, $P < 0.001$], and that the TS group performed worse overall [$F(1, 26) = 5.3$, $P = 0.029$].

Group Differences in Task-Related Regional Activations

Differences in task-related regional activations between the groups were tested using an SPM analysis. First-level contrasts comparing easy versus control, difficult versus control, and (easy + difficult) versus control were entered into two-sample *t*-tests. At a whole-brain corrected threshold of $P < 0.05$ family-wise error (FWE) corrected, there

TABLE II. Cluster locations

		TD								TS							
		Left				Right				Left				Right			
		Center of mass (mm)				Center of mass (mm)				Center of mass (mm)				Center of mass (mm)			
PPC split into *N* clusters	Cluster #	*x*	*y*	*z*	Size	*x*	*y*	*z*	Size	*x*	*y*	*z*	Size	*x*	*y*	*z*	Size
3	1	−51.7	−33.6	29.8	153	54.6	−34.2	29.7	178	−51.7	−33.6	29.8	153	54.6	−34.2	29.7	178
	2	−33.1	−49.7	51.9	245	34.4	−51.2	51.6	292	−33.1	−49.7	51.9	245	34.4	−51.2	51.6	292
	3	−43.3	−61.5	43.8	109	46.6	−60.3	43.9	85	−43.3	−61.5	43.8	109	46.6	−60.3	43.9	85
4	1	−50	−34.6	27.8	134	53.6	−33.7	28.4	153	−50	−34.6	27.8	134	53.6	−33.7	28.4	153
	2	−36.8	−48.2	54.3	7	56.8	−40.2	43.9	9	−36.8	−48.2	54.3	7	56.8	−40.2	43.9	9
	3	−43.7	−61.6	43.6	96	47.4	−60.6	43.4	76	−43.7	−61.6	43.6	96	47.4	−60.6	43.4	76
	4	−31.3	−51.3	52.1	158	32.5	−50.8	52.1	209	−31.3	−51.3	52.1	158	32.5	−50.8	52.1	209
5	1	−58.1	−38.2	36.6	35	62.3	−34.6	33.9	46	−58.1	−38.2	36.6	35	62.3	−34.6	33.9	46
	2	−35.6	−53.2	53.1	18	33.9	−59.3	50	37	−35.6	−53.2	53.1	18	33.9	−59.3	50	37
	3	−47.7	−34.7	26.9	111	46.4	−33.4	27.1	74	−47.7	−34.7	26.9	111	46.4	−33.4	27.1	74
	4	−44.5	−61.6	43.2	87	47.4	−60.7	43.2	73	−44.5	−61.6	43.2	87	47.4	−60.7	43.2	73
	5	−32.6	−47.2	52.4	128	32.7	−49.5	52.2	177	−32.6	−47.2	52.4	128	32.7	−49.5	52.2	177
6	1	−44.7	−32.9	26.9	72	48.8	−32.4	26.9	69	−44.7	−32.9	26.9	72	48.8	−32.4	26.9	69
	2	−19.6	−54.7	62.9	12	28.6	−43.3	57.5	2	−19.6	−54.7	62.9	12	28.6	−43.3	57.5	2
	3	−40.2	−60.4	50	1	46.8	−62.2	43.5	24	−40.2	−60.4	50	1	46.8	−62.2	43.5	24
	4	−31	−59.3	43.3	3	32	−67.3	50	2	−31	−59.3	43.3	3	32	−67.3	50	2
	5	−40.7	−39.5	45.4	52	36.1	−45.2	46.4	76	−40.7	−39.5	45.4	52	36.1	−45.2	46.4	76
	6	−45.3	−62.2	39.5	29	49.9	−47.4	25	5	−45.3	−62.2	39.5	29	49.9	−47.4	25	5

The extent of each cluster was defined by voxels that belong to the cluster in at least 60% of participants in the group. This table provides a description of the resulting clusters for analyses dividing PPC into 3–6 clusters.

were no significant differences between groups in any of these contrasts. We also performed a small-volume correction (height $P < 0.001$ and extent $P < 0.05$ FWE) in bilateral parietal cortex, and found no significant differences between groups in any of these contrasts. In order to compare differences in task-related activation with differences in network recruitment described later in this paper, the threshold for group comparisons was reduced to $P < 0.005$ uncorrected. At this threshold we found group differences in the contrast pooling easy and difficult JLO blocks, relative to control blocks, for TD > TS, in bilateral inferior parietal cortex (left: peaks at [−42, −38, 42] and [−28, −38, 42], $n = 209$, $Z = 3.07$; right: [36, −30, 38], $n = 9$, $Z = 2.71$). There were no differences in parietal cortex at this threshold for TS > TD.

Clustering Results

Voxels in the bilateral PPC ROI were grouped into clusters based on temporal correlation with the target ROI mask. For each cluster, and within each diagnostic group, voxel-wise maps were created showing the proportion of participants for which a given voxel belonged to that cluster. We define the extent of each cluster as the voxels that belong to the cluster in at least 60% of participants across the entire sample; size and center of mass for cluster divisions from 3 to 6 are shown in Table II. Figure 2a,b shows the spatial distribution of voxels for 3 clusters in the TD and TS groups; Figure 2d,e shows the spatial distribution of voxels for five clusters in the TD and TS groups. Clusters show bilateral symmetry and similar spatial distributions across the two groups. In the three cluster condition, the PPC divides into superior, inferior, and more posterior segments [Anderson et al., 2010; Mars et al., 2011]. At 6 clusters, more superior/anterior and more posterior/inferior segments split off the superior parietal clusters, and a more posterior cluster emerges from the inferior parietal cluster.

For up to six clusters, each cluster included voxels which were shared by at least 60% of participants across the entire sample. Within each cluster and at each voxel, significant differences in cluster membership between groups were evaluated, and the number of contiguous voxels showing significant differences were thresholded for extent using a permutation analysis. Significant differences in the spatial distribution of voxels belonging to specific clusters were identified, for 3–6 clusters (Fig. 2c,f; Table III).

Maps of voxels showing significant differences in cluster membership between groups were binarized and summed over the 3, 4, 5, and 6 cluster conditions. The resulting map in Figure 3 shows the number of analyses for which

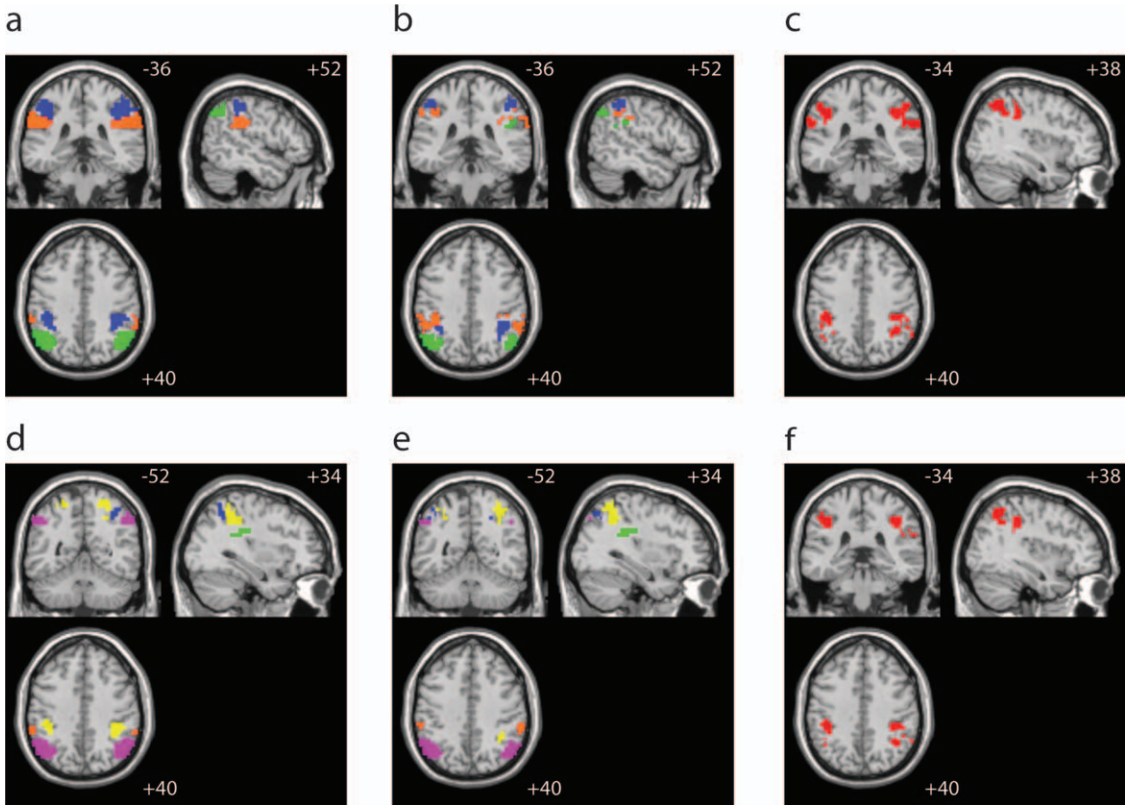

Figure 2.

Connectivity-based clustering of PPC voxels. PPC voxels were divided into *N* separate clusters in each participant. At the group level, clusters are defined as the set of voxels which belong to a given cluster for ≥60% of participants. Cluster sizes and centers of mass are listed in Table II. (**a**) TD and (**b**) TS groups with PPC voxels divided into three clusters. Color-coding relative to Table II: orange = 1, blue = 2, green = 3. (**c**) Voxels showing significant group differences in cluster membership for the 3-cluster case ($P < 0.05$ uncorrected) are shown in red. (**d**) TD and (**e**) TS groups with PPC voxels divided into five clusters. Color-coding relative to Table II: orange = 1, blue = 2, green = 3, magenta = 4, yellow = 5. (**f**) Voxels showing significant differences in cluster membership for the 5-cluster case ($P < 0.05$ uncorrected) are shown in red. [Color figure can be viewed in the online issue, which is available at wileyonlinelibrary.com.]

a given voxel was found to cluster significantly differently between groups; lighter colors indicate that a voxel was consistently found to cluster differently between groups, white voxels showed significant differences for each of the 3, 4, 5, and 6 cluster analyses. Regions of bilateral inferior parietal lobule (centered on [41, −35, 40] and [−41, −35, 42], 23 and 35 contiguous voxels, respectively), and posterior superior parietal lobule (centered on [43, −56, 50], 47 contiguous voxels) show consistent group differences independent of the number of clusters into which the PPC is divided.

Whole-Brain Correlation Patterns for Clusters

Representative time-courses from each cluster were entered into a whole-brain regression analysis, to identify which regions of the brain significantly correlate with each cluster across the whole group (TD+TS). The resulting whole brain correlation maps for five parietal clusters (cluster locations are shown in Fig. 4a) are shown in Figure 4b, illustrating that each cluster shows a unique pattern of correlation with voxels across the brain.

Connectivity Differences in Regions Showing Group Differences in Clustering

Left posterior superior parietal lobule [43, −56, 50] showed preferential correlations with lingual gyrus, bilateral calcarine sulcus, and superior temporal gyrus in the TD group, and middle frontal gyrus, SMA, paracentral lobule, and posterior right superior parietal gyrus in the TS group (Fig. 5a).

Bilateral supramarginal gyrus regions ([−41, −35, 40] and [41, −35, 40]) showed preferential connectivity with lateral occipitotemporal cortex (LOTC) bilaterally, and lingual gyrus regions in TD relative to TS participants (Fig.

TABLE III. Significant group differences in cluster membership

PPC divided into *N* clusters	Cluster #	Direction	Size	MNI coordinates (mm) X	Y	Z	*P* value
3	1	TS > TD	27	−41	−38	43	0.026
	1	TD > TS	32	59	−30	28	0.015
	1	TD > TS	23	−58	−32	31	0.027
	2	TS > TD	53	43	−55	50	0.003
	2	TD > TS	47	44	−35	44	0.006
	2	TD > TS	43	−42	−35	42	0.008
	3	TS > TD	30	58	−32	29	0.034
	3	TS > TD	32	−53	−33	30.8	0.03
	3	TD > TS	75	44	−54	48	0.006
4	2	TS > TD	15	39	−36	43	0.03
	3	TD > TS	38	43	−57	48	0.008
	4	TS > TD	24	44	−53	52	0.05
	4	TD > TS	27	40	−36	41	0.04
5	1	TS > TD	17	−42	−34	43	0.03
	1	TD > TS	26	54	−33	27	0.01
	3	TS > TD	31	58	−35	27	0.008
	4	TD > TS	40	45	−57	47	0.01
	5	TS > TD	37	39	−56	51	0.0005
	5	TD > TS	29	41	−36	42	0.005
	5	TD > TS	52	−36	−40	47	<0.0001
6	1	TS > TD	16	59	−28	32	0.03
	3	TD > TS	22	44	−51	50	.016
	4	TD > TS	15	−59	−35	34	0.02
	5	TS > TD	28	37	−53	54	0.006
	5	TD > TS	15	42	−34	39	0.03
	5	TD > TS	31	−41	−35	40	0.004

For analyses dividing PPC into 3–6 clusters, each cluster was compared between groups to identify differences in spatial extent. Here, we list sets of contiguous voxels showing significant differences in cluster membership between groups ($P < 0.05$), with an extent found to be significant at $P < 0.05$ using permutation analyses (P values listed are based on cluster size).

5b). Only white matter regions were more engaged in the TS > TD contrast.

To test for bilateral consistency in differential functional connectivity between SMG and LOTC, the timecourse from the voxel showing the peak group difference in left LOTC ([−54, −62, −8]) was entered into a similar whole-brain analysis. This analysis revealed group differences in the SMG with peaks bilaterally at [−40, −26, 36] ($Z = 4.49$, $N = 533$) and [48, −30, 54] ($Z = 4.15$, $N = 1042$), and thereby reinforces the finding of reduced functional connectivity between SMG and LOTC in TS.

Finally, to rule out the possibility that functional connectivity differences between SMG and LOTC were driven by processes related to the task, an additional whole-brain regression analysis using the timecourse from the left SMG peak [−41, −35, 40] was run using only resting segments at the beginning, middle, and end of the task (90 s total). The model in this case included only the voxel time course and motion regressors. This analysis also showed group differences in (TD>TS) in functional connectivity with peaks in LOTC bilaterally (peaks at [−56, −60, −6], $Z = 4.37$, $N = 439$; and [56, −50, −12], $Z = 3.94$, $N = 76$).

DISCUSSION

In the present study, we describe, to our knowledge, the first comparison of connectivity-based clustering of PPC in a clinical population relative to a typically developing control group. This analysis revealed broad similarities in connectivity-based clusters of parietal cortex in TS, a neurodevelopmental disorder known to affect parietal cortex development. However, we identified significant differences between groups in the spatial extent of selected clusters. These results imply that abnormal structural development of the PPC affects network recruitment of this region, which may have implications for cognitive performance. Clustering of voxels based on similar functional or anatomical connectivity, offers a means of understanding the spatial distribution of function in specific regions of the brain.

Interestingly, when the connectivity of regions which consistently clustered differently in TS were compared between groups, it was observed that the TS group showed reduced connectivity with regions involved in visual processing, including LOTC, lingual gyrus, and parieto-occipital regions. This is interesting in light of studies on the cognitive profile in TS, which have frequently described impairments in visuospatial processing. More specifically, a bilateral reduction in functional connectivity between a region of SMG and LOTC was observed in TS, which drove differences in clustering. LOTC has been implicated in motion processing [Tootell et al., 1995], object recognition [Grill-Spector et al., 1999], and perception of bodies or body parts [Downing et al., 2001, 2007]. Although previous studies of white matter differences in TS have indicated abnormalities in parieto-occipital and parieto-temporal pathways [Holzapfel et al., 2006; Molko et al., 2003, 2004], to our knowledge this is the first report to uncover differences in functional connectivity between these regions. This finding highlights the usefulness of the method employed in this study, as it was able to isolate regions showing different functional connectivity patterns, within a large reigon, which could then be interrogated using a seed-based approach.

It is possible that because a visuospatial task was used in this study, we were biased towards observing differences in recruitment of these areas. To control for this, a follow-up analysis was performed using only the resting segments of the task. This analysis showed similar group differences in functional connectivity between SMG and LOTC, suggesting that task-related activation differences are not solely responsible for the observed differences in functional connectivity, and that differences in underlying anatomical connectivity may be a common cause of functional connectivity differences during task and rest. In a recent study involving overlapping subject groups with

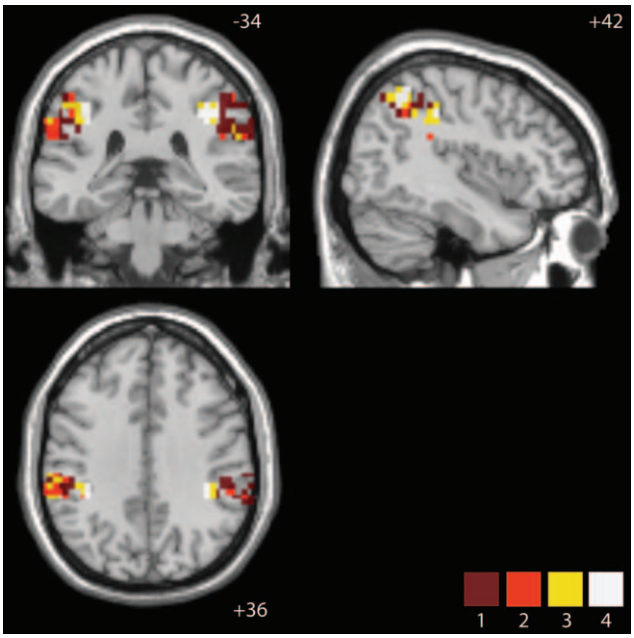

Figure 3.

Voxels showing group differences in clustering across multiple analyses. Maps of voxels showing significant differences in cluster membership for analyses dividing PPC voxels into 3, 4, 5, and 6 clusters were binarized and summed. From darker to lighter, colors indicate that a voxel clustered significantly different between groups across 1–4 separate analyses (i.e., division of PPC voxels into 3, 4, 5, or 6 clusters). Contiguous voxels in bilateral inferior parietal lobule ([−41, −35, 40] and [41, −35, 40]), and right superior parietal lobule [43, −56, 50] showed significant differences in all four cases (shown in white). [Color figure can be viewed in the online issue, which is available at wileyonlinelibrary.com.]

the sample described here, Yamagata et al. [2011] found that in a prepubertal sample of girls with TS, several white matter pathways involved in visuospatial processing showed reduced fractional anisotropy. These included left superior longitudinal fasciculus, splenium of the corpus callosum, and tapetum. These differences provide a putative anatomical basis for the differences in network recruitment of parieto-visual regions described here.

A potential source of the observed differences between the groups could be due to differences in performance on the task. For example, differences in connectivity could be engendered by one group paying less attention. However, while the performance difference between the groups was significant, the mean difference in accuracy was relatively small: 6% on the control task, 3% on the easy task, and 8% on the difficult task. It is therefore unlikely that group differences are related to differences in effort on the task. Furthermore, given that similar group differences in clustering were observed during the resting segments of the task, it seems unlikely that performance differences have a strong influence on our results. We also note that since we imposed a relatively high threshold for inclusion in this study (85% accuracy on the easy version of the task), our sample may not be representative of the full spectrum of individuals with TS. This may partly explain why group differences in activation were subtle relative to previous reports [Kesler et al., 2004].

The parcellation method described in the present study differs from previously published approaches. Anderson et al. [2010] used coordinates of peak correlation within each seed region, and clustered data from all participants at once. This approach has the advantage of identifying spatial clusters that are similar across a group of participants. However, this method makes it more difficult to identify group differences. In the present approach, we attempted to identify clusters that are similar across the

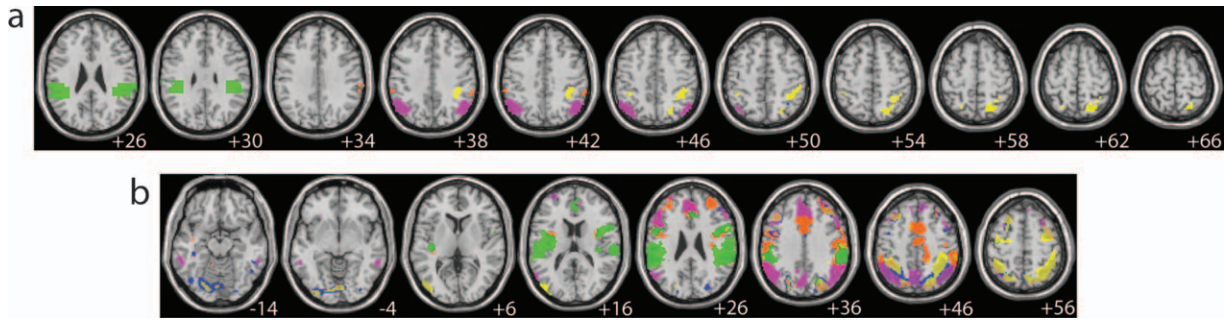

Figure 4.

Whole brain correlation maps for PPC clusters. (**a**) Clusters were defined across the entire group (TD+TS) as the set of voxels which belong to a given cluster in ≥60% of participants. (**b**) Representative time courses were extracted from each of the five clusters shown in (a) and entered into a whole-brain SPM analysis. The resulting contrast maps were entered into an F-contrast at the group-level and thresholded at $P < 0.05$ FWE-corrected over the whole brain. Voxels that significantly correlated with time courses from each of the five clusters shown in (a) are plotted in (b) using the same color coding. [Color figure can be viewed in the online issue, which is available at wileyonlinelibrary.com.]

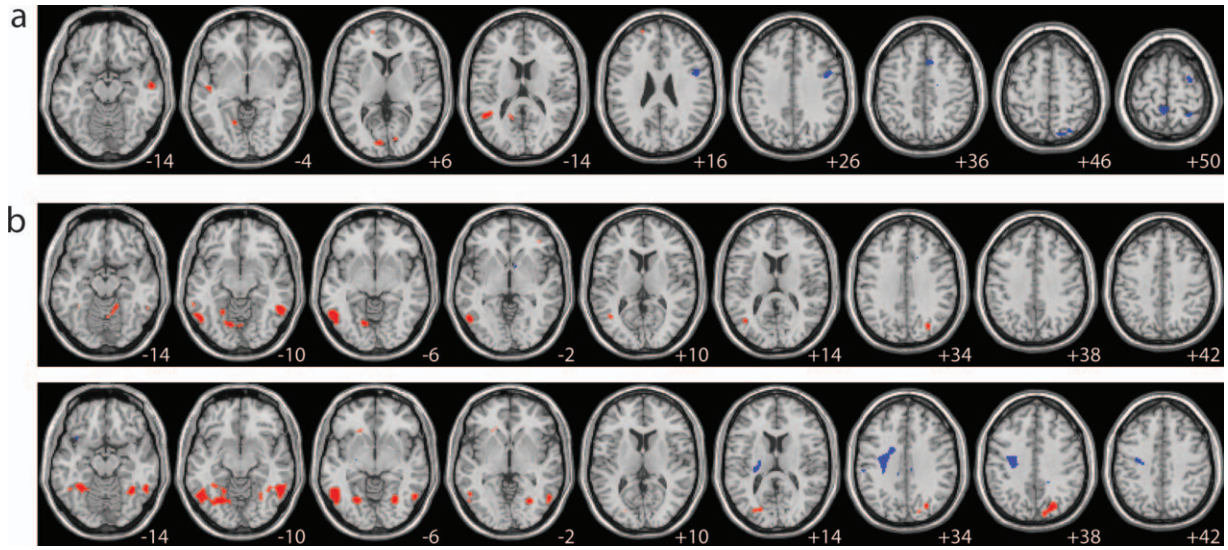

Figure 5.

Differences in whole brain correlation for voxels that cluster differently between groups. Time courses from voxels showing significant group differences in cluster membership for division into 3, 4, 5, and 6 clusters (shown in Fig. 3) were entered into whole-brain regression analyses and compared between groups. Results are shown at an exploratory threshold of $P < 0.001$ uncorrected: red = TD > TS, blue = TS > TD. (**a**) Group differences in correlation with right posterior parietal lobule [42, −56, 50]. (**b**) Group differences in correlation with right [40, −36, 40] (top) and left [−38, −36, 40] (bottom) inferior parietal lobule. [Color figure can be viewed in the online issue, which is available at wileyonlinelibrary.com.]

entire sample (clinical and typically developing control groups) in terms of connectivity to other regions, and then discern whether the spatial extent of these clusters was different between groups.

More generally, the connectivity-based clustering method described here differs from other methods that have been previously employed to assess group differences in functional connectivity. A common method is to test for differences in the amplitude of the zero-lag temporal cross-correlation between a seed region and another region or set of regions [Rogers et al., 2007]. Psychophysiological interaction methods [Friston et al., 1997] further test for task-related changes in inter-regional correlations. Comparing groups on the basis of spatial extent of clusters defined by connectivity does not provide any information about differences in the amplitude of inter-regional correlations, but rather is designed to ask whether there are functional networks that are absent or otherwise differently configured in the clinical comparison group. The assumption underlying both types of analyses is that connectivity differences likely reflect differences in underlying structural connectivity, however, with the connectivity clustering method one can test for connectivity differences in a large contiguous region, whereas seed-based connectivity methods require a specific a priori hypothesis about the chosen seed region. Another, related, approach to functional connectivity analyses is to build network models from connectivity information, which can be analyzed using graph theoretical measures [Achard et al., 2006]. Recent methods have been developed to facilitate statistical comparison of these models between diagnostic groups [Alexander-Bloch et al., 2012], and in future it would be interesting to apply these to Turner syndrome, to test whether at the whole-brain level, the posterior parietal cortex would stand out as a region with abnormal community membership.

The localization of clusters reported in the present study agrees with previously published reports for division of PPC into three clusters, which typically divide the PPC into superior, inferior and more posterior clusters [Anderson et al., 2010; Mars et al., 2011]. One methodological difference from the present study is that Mars et al. [2011] then subdivided these three clusters, whereas in the analysis described here, each level of clustering (e.g. 3, 4, or 5 clusters) was performed independently of the next. Mars et al. [2011] identified five clusters in inferior parietal lobule, from anterior to posterior: parietal operculum, anterior and posterior supramarginal gyrus, anterior and posterior angular gyrus. Similarly, five superior/IPS clusters were identified along the anterior to posterior axis. In the present study, when moving from three to six clusters, regions along the superior parietal/IPS cluster similarly split into more anterior and posterior segments.

In the present study, we were able to use functional connectivity measures to reliably identify six clusters in the lateral parietal cortex, which is fewer than the 10 which Mars et al. [2011] were able to identify using anatomical connectivity to parcellate the PPC. Several possible reasons may contribute to this difference. First, functional

connectivity is likely less specific than anatomical connectivity, for example two regions may show correlated activity, but weak or absent anatomical connectivity, due to similar task response, or due to shared anatomical connectivity with a third region. Second, in the Mars study connectivity with the seed region was calculated across the whole brain, then cross-correlations across the seed region were calculated and entered into the analysis. Since whole-brain connectivity information was used rather than a set of target regions, this analysis was potentially more sensitive. Third, we are studying a sample of children and pre-adolescents, as well as a clinical group, which may contribute to variability. The advantage of the present approach is that it was applied to $\sim$ 8 min of blocked design task data, whereas Mars et al. used a $\sim$ 45 min DTI protocol, which would be challenging to reliably obtain in a pediatric clinical population.

Anderson et al. [2010] used connectivity-based clustering of resting state data to demonstrate that attentional regions along the intraparietal sulcus are topographically organized. That is, sub-regions of the IPS showed stronger connectivity with auditory, sensorimotor, visual, and default mode regions. It is possible that in the present study, because we used a task rather than resting scan to calculate connectivity, we are biased towards detecting networks which are engaged by the visual task, and less sensitive to auditory or sensorimotor networks. In Anderson et al. [2010] each voxel in the brain was assigned to the cluster with which it maximally correlated. In the present study, we generated maps of regions showing significant correlations to each cluster, at the group level. We identified partially overlapping but also partially separable patterns of significant correlation with regions across the brain. These similarly included regions typically associated with attentional or resting networks, as well as visual, motor, and auditory regions.

In this study, we present an exploratory analysis of differences in connectivity of the PPC in Turner syndrome. There are several limitations associated with this study. The major limitation is relatively small sample-size, which resulted in reduced power to detect subtle differences in connectivity patterns. Another potential limitation is the use of a task-based scan rather than a resting-state scan, as has been typically employed in previous studies. The disadvantage of using a task-based scan in this context is that the resulting networks may be biased towards those recruited by the task. We attempted to use this to our advantage by using the regions modulated by the task to define a set of target regions in the connectivity analysis. Effectively, this means that we are looking for gradations in connectivity within the functional network defined by the task. This approach was effective in identifying consistent clusters across our sample, and the identified clusters seem qualitatively similar with those identified in previous studies [Anderson et al., 2010; Mars et al., 2011]. In future, it would be interesting to follow-up on this study using diffusion tractography or a full-length resting-state scan. Finally, as with many studies in clinical populations, we assume that data from a clinical population can be normalized into the same space as a TD group. If this assumption is violated, a potential interpretation of the observed group differences is that different anatomical regions are being compared between groups, rather than the same anatomical region showing different connectivity patterns in TS. However, our findings nonetheless indicate that variability in the structure of PPC results in differences in the extent of functional network recruitment in TS, whether due to variability in the functional connectivity of similar regions or due to differences in regional anatomy.

CONCLUSIONS

In conclusion, we present here a comparison of functional network recruitment of the PPC in Turner syndrome. It was found that while the PPC broadly divides into similar networks in TS and TD participants, several regions reliably showed differential clustering in TS. These differences related to differences in correlation with visual processing regions, an interesting finding in light of the visuospatial processing deficits frequently described in TS. The present study thus lays the groundwork for a more detailed investigation into the consequences of abnormal parietal cortex development, not only in terms of localized differences in activation, but also the dynamic interactions with other brain regions that are essential to cognitive function.

ACKNOWLEDGMENTS

The authors acknowledge the assistance from Kristen Sheau, Yaena Park, Matthew Marzelli, and Della Koovakkattu. The authors acknowledge support from the Canadian National Science and Engineering Research Council [SB], iCORE [SB], the National Alliance for Research on Schizophrenia and Depression (NARSAD) [FH], NICHD HD054720, and Lucile Packard Foundation for Children's Health (LPFCH), Spectrum Child Health, Clinical and Translational Science Award [FH], National Institute of Child Health and Human Development [5-R01-HD049653 to A.L.R.]; Chain of Love Foundation [to A.L.R.]; American Psychiatric Institute for Research and Education/Lilly Psychiatric Research Fellowship Award [to D.H.]; and National Institute of Mental Health [T32- MH19908 to A.L.R., D.H.].

REFERENCES

Achard S, Salvador R, Whitcher B, Suckling J, Bullmore E (2006): A resilient, low-frequency, small-world human brain functional network with highly connected association cortical hubs. J Neurosci 26:63–72.

Alexander-Bloch A, Lambiotte R, Roberts B, Giedd J, Gogtay N, Bullmore E (2012): The discovery of population differences in network community structure: New methods and applications to brain functional networks in schizophrenia. Neuroimage 59:3889–3900.

Anderson JS, Ferguson MA, Lopez-Larson M, Yurgelun-Todd D (2010): Topographic maps of multisensory attention. Proc Natl Acad Sci USA 107:20110–20114.

Benton AL, Varney NR, Hamsher KD (1978): Visuospatial judgment. A clinical test. Arch Neurol 35:364–367.

Bray S, Dunkin B, Hong DS, Reiss AL (2011): Reduced functional connectivity during working memory in Turner syndrome. Cerebr Cortex.

Brown WE, Kesler SR, Eliez S, Warsofsky IS, Haberecht M, Patwardhan A, Ross JL, Neely EK, Zeng SM, Yankowitz J, et al. (2002): Brain development in Turner syndrome: A magnetic resonance imaging study. Psychiatry Res 116:187–196.

Cutter WJ, Daly EM, Robertson DM, Chitnis XA, van Amelsvoort TA, Simmons A, Ng VW, Williams BS, Shaw P, Conway GS, et al. (2006): Influence of X chromosome and hormones on human brain development: A magnetic resonance imaging and proton magnetic resonance spectroscopy study of Turner syndrome. Biol Psychiatry 59:273–283.

Downing PE, Jiang YH, Shuman M, Kanwisher N (2001): A cortical area selective for visual processing of the human body. Science 293:2470–2473.

Downing PE, Wiggett AJ, Peelen MV (2007): Functional magnetic resonance imaging investigation of overlapping lateral occipitotemporal activations using multi-voxel pattern analysis. J Neurosci 27:226–233.

Fox MD, Snyder AZ, Vincent JL, Corbetta M, Van Essen DC, Raichle ME (2005): The human brain is intrinsically organized into dynamic, anticorrelated functional networks. Proc Natl Acad Sci USA 102:9673–9678.

Friston K, Buechel C, Fink G, Morris J, Rolls E, Dolan R (1997): Psychophysiological and modulatory interactions in neuroimaging. Neuroimage 6:218–229.

Glover GH, Law CS (2001): Spiral-in/out BOLD fMRI for increased SNR and reduced susceptibility artifacts. Magn Reson Med 46:515–522.

Good CD, Lawrence K, Thomas NS, Price CJ, Ashburner J, Friston KJ, Frackowiak RS, Oreland L, Skuse DH (2003): Dosage-sensitive X-linked locus influences the development of amygdala and orbitofrontal cortex, and fear recognition in humans. Brain 126:2431–2446.

Grill-Spector K, Kushnir T, Edelman S, Avidan G, Itzchak Y, Malach R (1999): Differential processing of objects under various viewing conditions in the human lateral occipital complex. Neuron 24:187–203.

Holzapfel M, Barnea-Goraly N, Eckert MA, Kesler SR, Reiss AL (2006): Selective alterations of white matter associated with visuospatial and sensorimotor dysfunction in turner syndrome. J Neurosci 26:7007–7013.

Honey CJ, Kotter R, Breakspear M, Sporns O (2007): Network structure of cerebral cortex shapes functional connectivity on multiple time scales. Proc Natl Acad Sci USA 104:10240–10245.

Hong D, Scaletta Kent J, Kesler S (2009): Cognitive profile of Turner syndrome. Dev Disabil Res Rev 15:270–278.

Kesler SR, Haberecht MF, Menon V, Warsofsky IS, Dyer-Friedman J, Neely EK, Reiss AL (2004): Functional neuroanatomy of spatial orientation processing in Turner syndrome. Cerebr Cortex 14:174–180.

Kim DH, Adalsteinsson E, Glover GH, Spielman DM (2002): Regularized higher-order in vivo shimming. Magn Reson Med 48:715–722.

Knops A, Thirion B, Hubbard EM, Michel V, Dehaene S (2009): Recruitment of an area involved in eye movements during mental arithmetic. Science 324:1583–1585.

Lawrence K, Kuntsi J, Coleman M, Campbell R, Skuse D (2003): Face and emotion recognition deficits in Turner syndrome: A possible role for X-linked genes in amygdala development. Neuropsychology 17:39–49.

Lewis JW, Beauchamp MS, DeYoe EA (2000): A comparison of visual and auditory motion processing in human cerebral cortex. Cerebr Cortex 10:873–888.

Lippe B (1991): Turner syndrome. Endocrinol Metab Clin North Am 20:121–152.

Mars RB, Jbabdi S, Sallet J, O'Reilly JX, Croxson PL, Olivier E, Noonan MP, Bergmann C, Mitchell AS, Baxter MG, et al. (2011): Diffusion-weighted imaging tractography-based parcellation of the human parietal cortex and comparison with human and macaque resting-state functional connectivity. J Neurosci 31:4087–4100.

Marzelli MJ, Hoeft F, Hong DS, Reiss AL (2011): Neuroanatomical spatial patterns in Turner syndrome. Neuroimage 55:439–447.

Mazaika P, Hoeft F, Glover G, Reiss A (2009): Methods and software for fMRI analysis for clinical subjects. Hum Brain Mapp Conference.

Mazzanti L, Cacciari E (1998): Congenital heart disease in patients with Turner's syndrome. J Pediatrics 133:688–692.

Molko N, Cachia A, Rivière D, Mangin JF, Bruandet M, Le Bihan D, Cohen L, Dehaene S (2003): Functional and structural alterations of the intraparietal sulcus in a developmental dyscalculia of genetic origin. Neuron 40:847–858.

Molko N, Cachia A, Riviere D, Mangin JF, Bruandet M, LeBihan D, Cohen L, Dehaene S (2004): Brain anatomy in Turner syndrome: Evidence for impaired social and spatial-numerical networks. Cereb Cortex 14:840–850.

Nelson SM, Cohen AL, Power JD, Wig GS, Miezin FM, Wheeler ME, Velanova K, Donaldson DI, Phillips JS, Schlaggar BL, et al. (2010): A parcellation scheme for human left lateral parietal cortex. Neuron 67:156–170.

Raznahan A, Cutter W, Lalonde F, Robertson D, Daly E, Conway GS, Skuse DH, Ross J, Lerch JP, Giedd JN, et al. (2010): Cortical anatomy in human X monosomy. Neuroimage 49:2915–2923.

Rogers BP, Morgan VL, Newton AT, Gore JC (2007): Assessing functional connectivity in the human brain by fMRI. Magn Reson Imaging 25:1347–1357.

Silver MA, Kastner S (2009): Topographic maps in human frontal and parietal cortex. Trends Cogn Sci 13:488–495.

Stochholm K, Juul S, Juel K, Naeraa RW, Gravholt CH (2006): Prevalence, incidence, diagnostic delay, and mortality in Turner syndrome. J Clin Endocrinol Metab 91:3897–3902.

Swisher JD, Halko MA, Merabet LB, McMains SA, Somers DC (2007): Visual topography of human intraparietal sulcus. J Neurosci 27:5326–5337.

Todd JJ, Marois R (2004): Capacity limit of visual short-term memory in human posterior parietal cortex. Nature 428:751–754.

Tootell RBH, Reppas JB, Kwong KK, Malach R, Born RT, Brady TJ, Rosen BR, Belliveau JW (1995): Functional-analysis of human MT and related visual cortical areas using magnetic-resonance-imaging. J Neurosci 15:3215–3230.

Tzourio-Mazoyer N, Landeau B, Papathanassiou D, Crivello F, Etard O, Delcroix N, Mazoyer B, Joliot M (2002): Automated anatomical labeling of activations in SPM using a macroscopic anatomical parcellation of the MNI MRI single-subject brain. Neuroimage 15:273–289.

Uddin LQ, Supekar K, Amin H, Rykhlevskaia E, Nguyen DA, Greicius MD, Menon V (2010): Dissociable connectivity within human angular gyrus and intraparietal sulcus: Evidence from functional and structural connectivity. Cerebr Cortex 20:2636–2646.

Wechsler D (2003): Wechsler Intelligence Scale for Children, 4th ed. Technical and Interactive Manual. San Antonio, TX: The Psychological Corporation.

Yamagata B, Barnea-Goraly N, Marzelli MJ, Park Y, Hong DS, Mimura M, Reiss AL (2011): White matter aberrations in prepubertal estrogen-naive girls with monosomic Turner syndrome. Cerebr Cortex, in press, doi:10.1093/cercor/bhr35.